PROCEEDINGS OF THE ROYAL SOCIETY A MATHEMATICAL, PHYSICAL & ENGINEERING SCIENCES

The Dissociation of Water Vapour Behind Shock Waves

J. B. Homer and I. R. Hurle

Proc. R. Soc. Lond. A 1970 **314**, 585-598
doi: 10.1098/rspa.1970.0024

Proc. Roy. Soc. Lond. A. **314**, 585–598 (1970)
Printed in Great Britain

The dissociation of water vapour behind shock waves

By J. B. Homer and I. R. Hurle

Shell Research Ltd, Thornton Research Centre, P.O. Box 1, *Chester, CH* 1 3*SH*

(*Communicated by T. M. Sugden, F.R.S.—Received* 13 *June* 1969)

The dissociation of water vapour in dilute (< 7 %) mixtures with argon has been studied behind shock waves. The growth of OH concentration in the initial stages of dissociation was followed using a short-duration flash-absorption technique which recorded the OH (0, 0) band with high resolution.

Profiles of OH concentration were constructed for various conditions of temperature and concentration and a computer analysis was used to match these profiles to a proposed reaction sequence. The results indicate that basically the decomposition proceeds by the reaction

$$H_2O + M \xrightarrow{k_{1,M}} H + OH + M,$$

and rate constants for this reaction were determined over a temperature range of 2570 to 3290 K with M = Ar and H_2O. The overall rate equation can be expressed as

$$k_{1,M}[M] = A\{[Ar] + \eta[H_2O]\}T^{-N}\, e^{-D_0/RT}$$

with D_0 being 494 kJ mol^{-1} (118 kcal mol^{-1}), and the calculated parameters being:

$$A = (4.0 \pm 0.5) \times 10^{23} \text{ cm}^3 \text{ mol}^{-1} \text{ s}^{-1}, \quad \eta = 20 \pm 7, \quad N = 2.2 \pm 0.8.$$

This result, together with the equilibrium constant of the reaction, provides an assessment of the rate of the reverse process, the recombination of H and OH, which in conjunction with previous assessments in flames and shock tubes presents a unified and most consistent set of rate data over a wide temperature range.

1. Introduction

Two previous shock-tube studies of the decomposition of water vapour in argon have been published. Bauer, Schott & Duff (1958) followed the rate of appearance of OH by monitoring the absorption of ultraviolet light from a long duration, water-discharge flash. They reported an extremely low activation energy (192 kJ mol^{-1}, 46 kcal mol^{-1}) for the rate of appearance of OH, compared with a value of D_0 of 494 kJ mol^{-1} (118 kcal mol^{-1}) for the direct dissociation of water into H and OH, and to account for this proposed a peroxide mechanism for the decomposition. Olschewski, Troe & Wagner (1966) used much more dilute (< 0.2 %) water–argon mixtures and, by observing the infrared emission from water, determined an activation energy of 439 kJ mol^{-1} (105 kcal mol^{-1}) for the rate of disappearance of water, which is consistent with the simple dissociation process:

$$H_2O + M \rightarrow H + OH + M. \qquad (1)$$

The reverse of this process, the recombination of H and OH radicals, is of particular importance in controlling the rate of heat release in the final stages of flame systems, and differing values of its rate constant in the literature are based on

studies of the complex situations that exist in flames. Recent shock-tube studies on H_2–O_2 mixtures by Getzinger (1966; Getzinger & Blair 1968) have pointed towards an abnormally high efficiency for water compared to an inert gas, argon, as the third body, M, in the recombination reaction.

In order to resolve the situation we have re-examined the decomposition of water in dilute (< 7 %) mixtures with argon in a shock tube, and have determined the rate constants of the dissociation by reaction (1) over a temperature range of 2570–3290 K, with special reference to the efficiency of argon and water as M in the dissociation. By using the equilibrium constant in the calculation, the rate of the recombination process has been assessed from the dissociation rate and a comparison made with rates previously reported.

2. Experimental

The dissociation of water was initiated by the impact of a shock wave, and the subsequent growth of OH followed by a flash-absorption technique, similar in principle to that used by Gaydon, Kimbell & Palmer (1963). A flash tube giving light of a few microseconds duration was triggered by the shock to fire at a selected time after the shock wave passed an observation station. A high resolution absorption spectrum of the hot gas was recorded, and the $^2\Sigma^+ \leftarrow {}^2\Pi$ (0, 0) band system of OH in the region of 310 nm was analysed to give the concentration of OH at that selected time. Repeated shock experiments at different times of observation enabled the growth profile of OH to be constructed for various conditions of temperature and concentration.

The technique of taking a resolved spectrum, rather than of photometrically recording a specific band, has the advantage of eliminating ambiguities that might arise from spectral interference from other species.

The shock tube

The shock tube was the 10.2 cm internal diameter stainless steel tube as described previously by Hurle, Jones & Rosenfeld (1969). The driver gas was cold hydrogen at 1.72 to 5.17 MN m^{-2} (250 to 750 lbf/in^2) and the test gas, at pressures of 5.34 to 20.0 kN m^{-2} (40 to 150 Torr) was 0.25 to 7 % water vapour in argon. The double diaphragm facility in this shock tube, with its buffer section separating the driver and test sections, was found to be especially valuable in this work, since it allowed predictable shock temperatures to be reproduced within 1 %. Melinex diaphragms of multiple thicknesses, 0.18 to 1.14 mm, were used. Since these suffered partial fragmentation on bursting, the bore of the shock tube was cleaned before each shock experiment.

The conditions of temperature and density behind the shock wave were computed from the shock velocity, measured on a raster oscilloscope which recorded the signals from seven thermal resistance gauges spaced over a 3 m length of the tube. Shock velocity attenuation of less than 1 % per metre was encountered, and

the shock velocity at the pertinent positions in the tube were obtained to an accuracy of $\pm 0.2\,\%$ by graphical interpolation. This gave an uncertainty in the computed temperature of less than ± 10 K.

Gas handling

The adsorption of water vapour on the walls of the shock tube and mixing vessel could lead to uncertainties in the initial composition of the gas, and this was confirmed in preliminary experiments using tritiated water. Accordingly, special techniques were developed to fill the tube with known water–argon mixtures.

Argon of 99.995 % purity and water vapour were mixed in a 50 l Pyrex vessel. After the tube had been evacuated to 1.33 mN m^{-2} (10^{-5} Torr), the mixture was allowed to flow slowly through it and an in-series 2 l Pyrex sampling section thereby allowing the water content of the surface and gas phase to equilibrate. The pressure of gas in the shock tube was kept as close as possible to the finally required pressure during this operation. The flow was stopped after about 10 min, by which time the volume of the shock tube had been displaced approximately twice, and the sampling section and shock tube were isolated. The shock experiment was then performed. A sample of unshocked gas was subsequently analysed by pumping it through a helical trap submerged in liquid nitrogen to freeze out the water. The trapped ice was allowed to evaporate back into the sampling section, and the pressure of water vapour measured at room temperature on an oil manometer. The result was converted to a percentage content of water in the original gas.

Vapour pressures of water could be measured to ± 4.0 N m^{-2} (0.03 Torr) on the oil manometer. Since this accuracy could lead to excessive error for mixtures containing less than 1 % water, higher sensitivies were obtained for these by closing off part of the sampling system before the ice was evaporated; the volume of the remaining section gave a measured amplification factor of ten.

Spectroscopic technique

The basis of the spectroscopic technique for recording the OH absorption spectra was the production of a continuum flash of short duration ($\sim 3\,\mu$s) compared with the time scale (~ 2 ms in particle coordinates) of the reaction. A flash tube of the type described by Garton (1961) was used. A 320 J (8 kV, 10 μF) flash discharge in a 133 mN m^{-2} (10^{-3} Torr) pressure of helium was triggered, after suitable delay, from one of the thermal resistance velocity gauges. The light pulse was of 3 μs duration at half intensity and had a rise time to peak light output of 2 μs. The image of the flash originating from the centre of the discharge was focused centrally in the shock tube, and then refocused on to a 10 μm slit of a Bausch & Lomb 1.5 m stigmatic grating spectrometer. The optics were arranged so that the light uniformly filled this entrance slit. The grating (450 lines/mm) was operated in the second order, and by using quartz optics throughout, and Ilford 5G91 film, the spectral region around $\lambda = 310$ nm was recorded. The uniform

PROCEEDINGS OF THE ROYAL SOCIETY A MATHEMATICAL, PHYSICAL & ENGINEERING SCIENCES

continuum of the flash in this region was slightly impaired by the absorption lines from the aluminium in the flash tube. These appeared as broad but weak perturbations of the continuum, and did not effect the accuracy of measurement of the OH absorption lines.

The dispersion of the spectrometer was 0.75 nm/mm. A Hilger & Watt scanning microdensitometer, which had a spacial resolution of 1 μm, was used to translate the film records into microdensitometer traces. The spectral resolution of the final traces was better than 100 pm, which is sufficient to resolve the rotational line structure of the OH (0, 0) band. A typical absorption photograph and microdensitometer record are shown in figure 1.

For each shock, the emission from excited OH also was observed through a quartz window, set perpendicular to and in the same plane as the two windows used for the absorption. The emission from the centre of the shock tube was focused on to the entrance slit of a Spex grating spectrometer which was tuned to monitor the OH $^2\Sigma^+ \rightarrow {}^2\Pi$ emission at 306.4 nm with a band width of 2.5 nm. As a check on the shock-tube time coordinate, the signal from a photomultiplier detector was recorded on an oscilloscope together with a time signal from one velocity gauge. The time at which the absorption flash fired was recorded on this trace as a sharp peak from scattered light and electromagnetic pick-up from the flash. The OH emission was confused by a small continuum emission from the hot gas, and generally made examination for the origin of the excited OH unprofitable. These observations, however, served as a check on the quality of the shock over the complete time scale of reaction and as a measure of the time between the start of dissociation and the point at which the absorption spectrum was taken. An additional check on this time was obtained from the raster trace recording the shock velocity, which also recorded the electrical disturbance from the flash discharge. The delay time was thus measured to within 1 μs, and was adjusted to take into account the finite width of the flash.

3. Analysis and calibration of OH absorption

In order to minimize overall errors in film densitometry, seven separate spectra were recorded on each film by using a Hartmann diaphragm at the entrance slit of the spectrometer. Each absorption film was standardized to a curve of optical density against light intensity by utilizing three spectra positions for recording the flash intensity through calibrated neutral density filters. The remaining four positions on the film recorded the OH absorption from separate shocks, and the peak heights of the rotational lines of the corresponding microdensitometer traces were converted to intensities of absorption.

The temperature of OH was calculated, for several shocks, from the intensity distribution of the rotational lines. Within the error of this calculation ($\pm$ 200 K), the temperature corresponded to the bulk gas temperature computed from the shock properties; this showed that OH was effectively rotationally equilibrated.

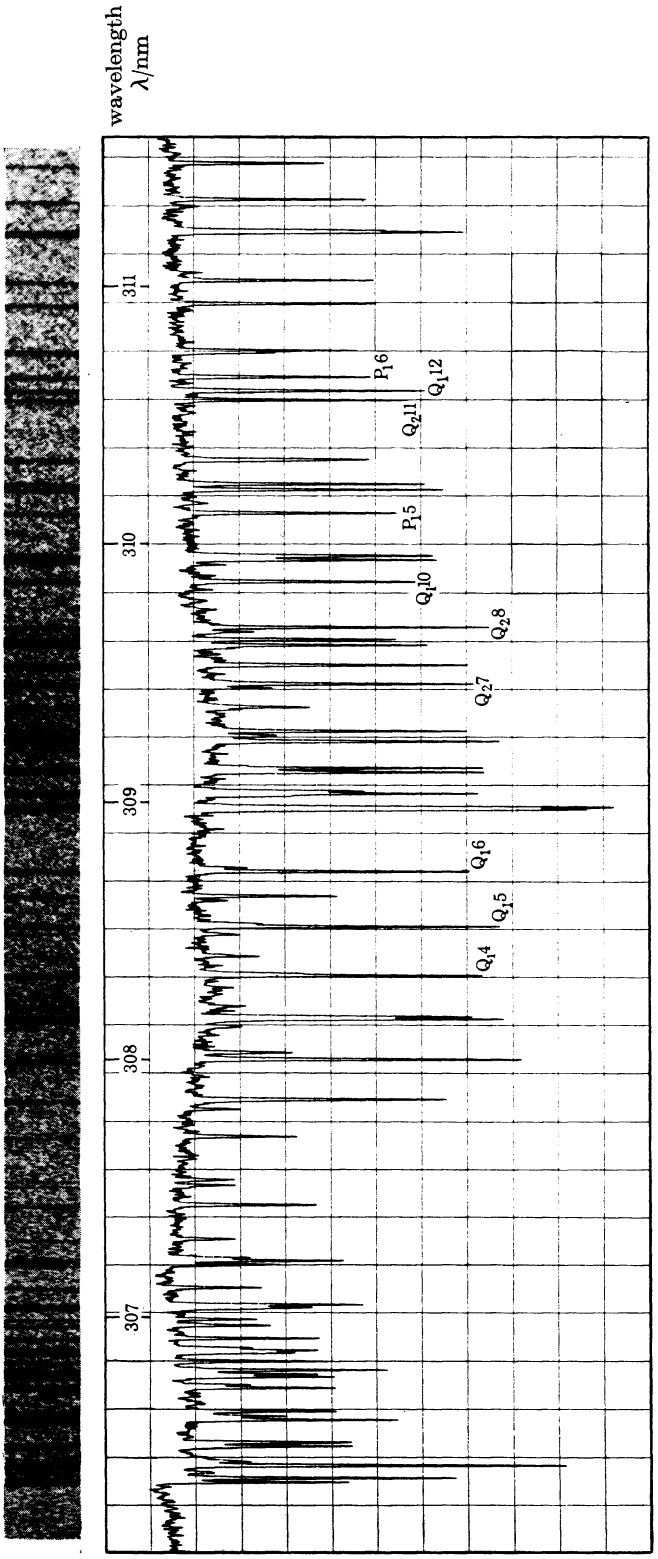

FIGURE 1. An absorption photograph and microdensitometer trace of a portion of the OH (0, 0) absorption band. The assigned rotational lines are those used in this work to represent the intensity of absorption. [OH] = 45 nmol cm^{-3}; T = 2770 K.

After initial tests, it was found that ten rotational lines of the OH (0, 0) band were sufficient to represent the total intensity of absorption. They were chosen as well isolated and unblended lines of medium intensity, corresponding to transitions from rotational levels whose populations varied little with temperature. This last criterion required, at these temperatures, that the transitions involved K values of around 10. In fact those lines chosen (figure 1) had K values from 4 to 12 and, on average, had a calculated slight negative dependence on temperature which gave rise to a deviation of less than 8 % in the line intensities over the temperature range examined. This was taken into account when these intensities were converted to absolute concentrations of OH.

The calibration of the intensity of the absorption spectrum against the absolute concentration of OH was accomplished by shock heating water–argon mixtures and by recording absorption spectra sufficiently late in the dissociation to ensure chemically equilibrated concentrations of OH. The theoretical concentration at equilibrium was computed from the shock condition and from the thermodynamic properties of all species likely to be present. Reasonable assurance that the chemical system had reached equilibrium by the time the calibration flash was fired was obtained by varying the time of firing and confirming that the OH absorption had reached an effectively constant intensity with time. This had additional confirmation in a computer analysis of the variation of radical species with time, a

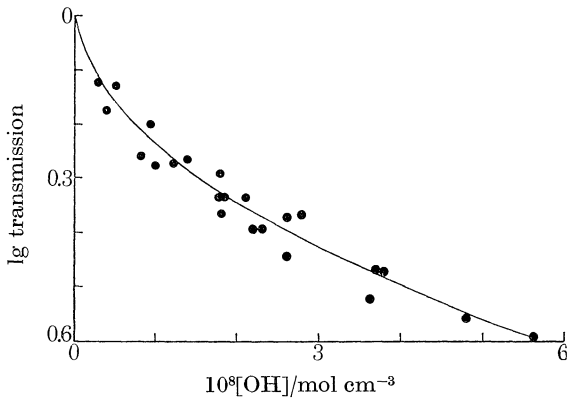

FIGURE 2. Calibration data for the mean absorption of the ten selected rotational lines of the OH absorption.

preliminary value for the rate of dissociation of water and preferred values, quoted by Schofield (1967), being used for the rates of other reactions known to exist in this system. These calculations showed that OH had reached a concentration that was within 5 % of the equilibrium value in the time available.

By varying the percentage of water from 0.25 to 5 % in argon, a calibration plot was constructed of OH concentration against the logarithm of the transmission (figure 2). It is not linear as Beer's law would require, the logarithm of the transmission tending to follow a square root dependence on OH concentration, and this

basically was the form of the mean line drawn through the individual points of the calibration curve. This behaviour is probably due to the relatively high concentrations of OH met with in this work, rather than to the lack of resolution of the absorption spectra. From data of line widths recently obtained for this spectra by Engleman (1969) for a variety of broadening gases, the total line width (combined collisional and Doppler) for the conditions used in the present studies is typically 100 pm. The Doppler width is predominant under these conditions, and this is consistent with our observations that for constant temperature and OH concentration no variation in line-peak absorption was detected over the range of total pressures used.

4. Calculation of the rate of dissociation

Eleven different sets of conditions of temperature and concentration (table 1) were examined and, for each, at least six points were produced on a plot of OH concentration against time, generally restricted to the initial 20 % of reaction. The experimental conditions within each set varied slightly, and the plots of OH concentration against time (the slight fall in temperature, < 50 K, due to chemical reaction being taken into account) were normalized to mean frozen conditions of temperature and concentration, by using preliminary values for the dependence of the initial slope of the plots on these two variables.

Table 1. Mean values of $k_{1,\mathrm{M}}[\mathrm{M}]$ for the various conditions of temperature and concentration

T/K	10^5[Ar]/mol cm^{-3}	10^7[H_2O]/mol cm^{-3}	$k_{1,\mathrm{M}}$ [M]/s^{-1}
3290	0.85	0.87	930
3190	0.87	2.60	950
3060	0.87	4.42	550
3050	1.06	1.03	440
2950	1.06	2.12	280
2930	1.09	3.24	290
2860	3.16	2.03	330
2830	1.07	5.20	210
2760	1.07	7.60	120
2700	1.27	3.26	60
2570	1.46	3.28	30

A preliminary assessment of the apparent activation energy for the initial rate of formation of OH was greater than 420 kJ mol^{-1} (100 kcal mol^{-1}), and this pointed towards the process being controlled by the reaction

$$\mathrm{H_2O + M} \xrightarrow{k_{1,\mathrm{M}}} \mathrm{H + OH + M} \qquad (1)$$

rather than by the peroxide mechanism that was proposed by Bauer *et al.* (1958). However, some of the OH profiles showed strong curvature early in the reaction which could not be accounted for solely by the reverse of reaction (1). To account

for this strong curvature and to give a more reliable determination of rate of reaction (1), additional reactions were therefore considered.

Reaction (1) will be followed by a series of low-energy, bimolecular atom-transfer reactions that have been previously recognized in the H_2/O_2 system:

$$H + H_2O \rightleftharpoons H_2 + OH, \tag{2}$$

$$H + OH \rightleftharpoons H_2 + O, \tag{3}$$

$$O + H_2O \rightleftharpoons OH + OH, \tag{4}$$

$$O + OH \rightleftharpoons H + O_2. \tag{5}$$

All these reactions will contribute to the OH profile. The selected values from Schofield (1967) for the forward and reverse rates of reactions (2) to (5) were used in computer calculations carried out to construct the profiles of all species involved under each experimental condition, and values of $k_{1,M}[M]$ were calculated for each experimental point. An example in which a computed OH profile is drawn

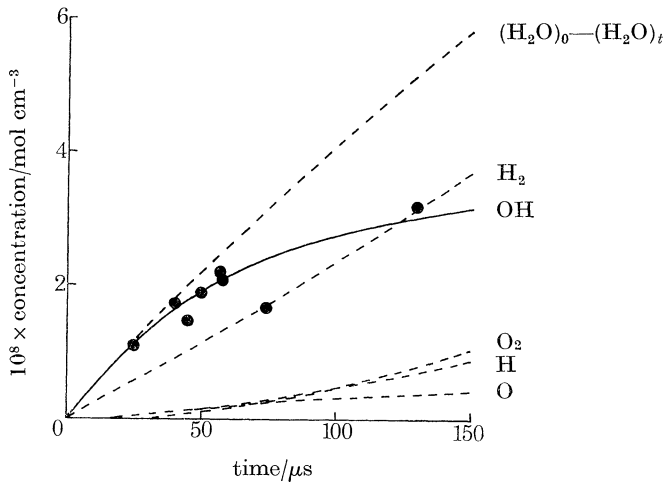

FIGURE 3. An example of an experimentally determined OH profile, and the computed profile using $k_{1,M}[M] = 550\ s^{-1}$. The computed profiles of the other species present are also shown. ($T = 3060$ K; [Ar] = 8.7 μmol cm^{-3}; $[H_2O]_0 = 0.44$ μmol cm^{-3}.)

through a set of experimental points is shown in figure 3, together with the computed profiles of the other species present. It followed from such calculations that the H atom concentration was too low in the early stages to allow the reverse of reaction (1) to proceed to any significant extent. It also followed that as reaction (2) is very fast and reactions (3) to (5) very slow compared with reaction (1), the computed values of $k_{1,M}[M]$ were only slightly affected by quite large variations in the inserted rates of reactions (2) to (5), and that the values of $k_{1,M}[M]$ were essentially half those calculated from the initial rate of production of OH on the assumption that the process was solely reaction (1). Although the dissociation of

OH itself must occur, estimates (Jenkins, Yumlu & Spalding 1966) of the rate for this process would indicate that the loss of OH by this step would be insignificant in the present treatment.

To simplify the presentation of the results in this paper, mean values of $k_{1,\mathrm{M}}[\mathrm{M}]$ were also evaluated for each set of experimental conditions and are presented in table 1. However, in the following section the 70 individually determined values of $k_{1,\mathrm{M}}[\mathrm{M}]$ were used in the anlysis in order to include the total error in the final formulations.

5. Interpretation of results

The results can be explained on the basis of the dissociation process, reaction (1). Olschewski *et al.* (1966) interpreted their work on the basis of the third body, M, being exclusively argon, which was valid since the water concentrations they used were very low ($< 0.2\,\%$). The water concentrations in the present work are much higher, so that the effect of water as a collision partner will be more evident.

The data were therefore unified by using a sum of two Arrhenius equations, corresponding to rates of reaction (1), with M being argon and water, and having an assumed common exponential term but differing collisional efficiencies:

$$k_{1,\mathrm{M}}[\mathrm{M}] = A\{[\mathrm{Ar}]+\eta[\mathrm{H_2O}]\}\mathrm{e}^{-B/T} \qquad \text{(i)}$$

where $\eta = k_{1,\mathrm{H_2O}}/k_{1,\mathrm{Ar}}$. A computer fit to this equation gave the values

$$A = (1.1 \pm 0.2) \times 10^{15}\ \mathrm{cm^3\ mol^{-1}\ s^{-1}},$$
$$\eta = 20 \pm 7,$$
$$B = (5.29 \pm 0.24) \times 10^4\ \mathrm{K^{-1}}.$$

The stated errors in these, and in subsequent values, are the standard 95 % confidence limits.

The fit of these values to the experimental points is demonstrated in two plots: figure 4 shows the variation of $k_{1,\mathrm{M}}[\mathrm{M}]/[\mathrm{Ar}]$ with $[\mathrm{H_2O}]/[\mathrm{Ar}]$ at a mean temperature of 2930 K (this plot yielding $k_{1,\mathrm{Ar}}$ from the intercept and $k_{1,\mathrm{H_2O}}$ from the slope for this particular temperature) and figure 5 the temperature dependence of the function $k_{1,\mathrm{M}}[\mathrm{M}]/\{[\mathrm{Ar}]+20[\mathrm{H_2O}]\}$.

The value of B is equivalent to an apparent activation energy of 439 kJ mol^{-1} (105 kcal mol^{-1}). The assumption that the temperature-dependence on k_1 is the same whether M is water or argon is not necessarily true. However, the experimentally available temperature range was too restrictive to allow an accurate separation of the two apparent activation energies; the data indicates that they differ by no more than 42 kJ mol^{-1} (10 kcal mol^{-1}).

A reformulation after the style of the classical theory of unimolecular decomposition was also carried out, and a computer fit to the equation:

$$k_{1,\mathrm{M}}[\mathrm{M}] = A\{[\mathrm{Ar}]+\eta[\mathrm{H_2O}]\}T^{-N}\,\mathrm{e}^{-D_0/RT}, \qquad \text{(ii)}$$

with an inserted value of D_0 of 494 kJ mol^{-1} (118 kcal mol^{-1}), yielded the values

$$A = (4.0 \pm 0.5) \times 10^{23} \text{ cm}^3 \text{ mol}^{-1} \text{ s}^{-1},$$
$$\eta = 20 \pm 7,$$
$$N = 2.2 \pm 0.8.$$

The two formulations gave equally good fits with the experimental results. Notably, the value of η was unaffected by the change to the different temperature function.

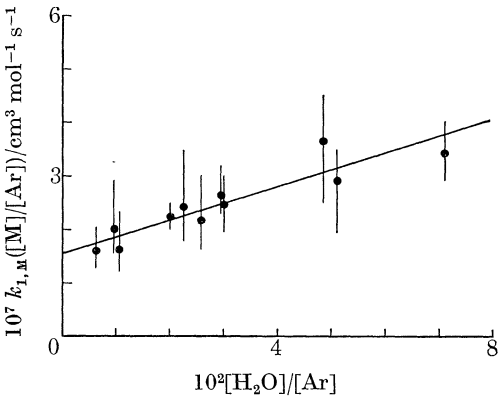

FIGURE 4

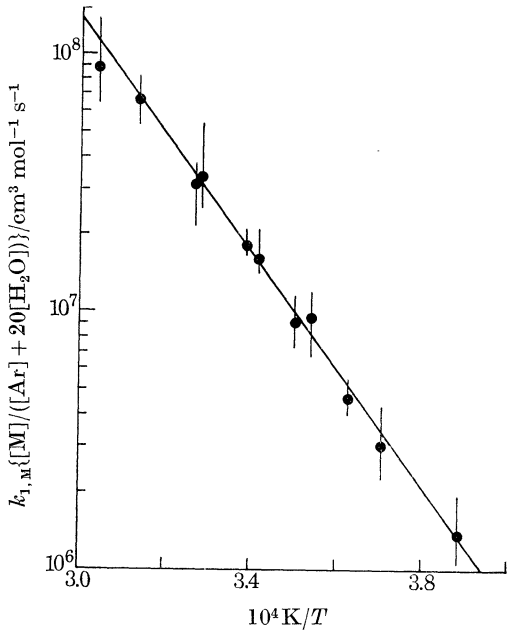

FIGURE 5

FIGURE 4. The dependence of $k_{1,M}[M]/[Ar]$ on $[H_2O]/[Ar]$, all data being standardized to a mean temperature of 2930 K. The points represent the mean values of $k_{1,M}[M]$ of table 1 and the error bars, the *total* spread of the individual data points.

FIGURE 5. Temperature dependence of the function $k_{1,M}[M]/\{[Ar] + 20[H_2O]\}$. The points and error bars have the same meaning as those in figure 4.

6. Discussion

The apparent activation energy determined from equation (i) is 439 ± 21 kJ mol^{-1} (105 ± 5 kcal mol^{-1}), and this is about 54 kJ mol^{-1} (13 kcal mol^{-1}) lower than the bond dissociation energy of water. The experimental results have been correlated on the supposition that the work has examined the low-pressure region of unimolecular decomposition, so that this energy deficit can be explained within the context of the classical theory of unimolecular kinetics by equation (ii). From this,

the value of N of 2.2 ± 0.8 indicates a comparatively large temperature dependence for the pre-exponential term. However, similar values have been reported for high temperature dissociations, notably in the work of Appleton, Steinberg & Liquornik (1968) on the dissociation of nitrogen, and Troe & Wagner (1967) have recently reviewed the field of unimolecular decompositions and have discussed this situation from a theoretical point of view.

There is a large difference between the efficiencies of water and argon as the collisional partners in the dissociation. Such high efficiencies of the dissociating molecule, when itself a collisional partner, have been previously reported for some systems, for example, for halogens, in the work of Christie, Harrison, Norrish & Porter (1955) and Britton (1960), where a complex intermediate is thought to be formed. It is plausible that the H_2O–H_2O collision could be particularly effective in forming a collisional complex which would facilitate the dissociation, especially if the strong polar forces were still useful at these high temperatures.

Since the rate of vibrational relaxation of water is expected to be very fast compared with the rates of dissociation reported here, the dissociation will not be retarded significantly by a vibrational repopulation process. It is therefore assumed that the equilibrium constant for the reaction can be used, without modification, to assess from the determined rates of the dissociation the rates of the reverse process:

$$H + OH + M \xrightarrow{k_{-1,M}} H_2O + M. \qquad (-1)$$

A comparison between the results of this work and those of other workers for the dissociation reaction is shown in figure 6. The agreement with the values of $k_{1,Ar}$ of Olschewski *et al.* (1966) is very good, especially in the temperature-dependence of the rate constants; their absolute magnitudes of the rates are about a factor of two lower than those reported here. The results disagree with those of Bauer *et al.* (1958) who presented a much lower activation energy (192 kJ mol^{-1}, 46 kcal mol^{-1}) than that shown by the data in figure 6 but, however, gave insufficient data to enable a reassessment of the individual rates as interpreted in the present paper.

The extrapolation to lower temperatures using equation (ii), shown as the broken lines in figure 6, correlates very well with the rate constants calculated from the rates of the reverse process, reaction (-1), which have been determined in previous flame and shock-tube studies. The extrapolation from equation (ii) assumes than N is invariant with temperature. Since N would be expected to decrease towards lower temperatures, the extrapolated values are probably slightly overestimated.

The overall temperature dependence of the rate constants plotted in figure 6 is dominated by the exponential term. A plot in terms of the rates for the reverse, recombination reaction (-1) is a more sensitive way of demonstrating the temperature dependence of the pre-exponential term. In figure 7, the rates of the recombination reaction as calculated from the present results, using the equilibrium constant of the reaction, are compared with those reported by other workers. The extrapolation to lower temperatures again uses equation (ii).

There is good agreement with the previous shock-tube work on H_2–O_2 mixtures of Getzinger (1966) and of Schott & Bird (1964) for which M = Ar, and particularly with Getzinger & Blair who also reported the ratio $k_{-1,H_2O}/k_{-1,Ar}$ as being about 20.

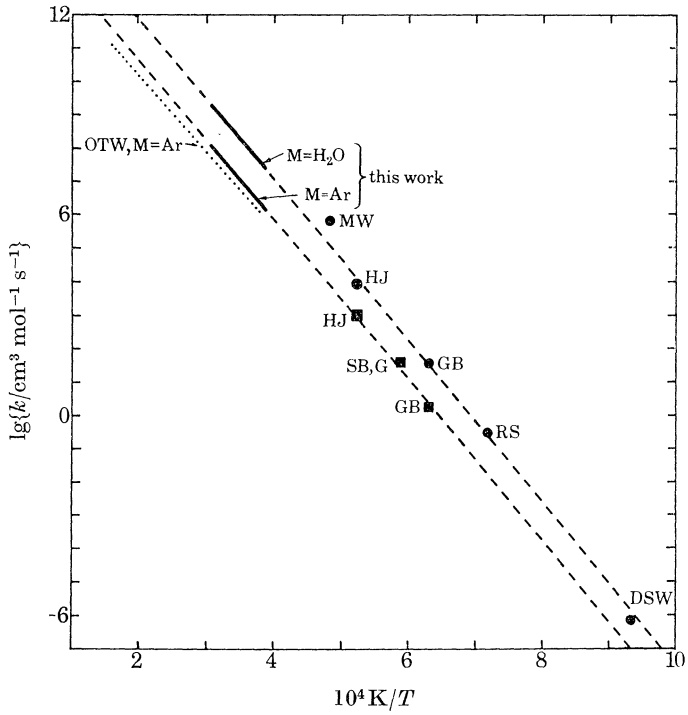

FIGURE 6. Rate constants for the reaction: $H_2O + M \rightarrow H + OH + M$, as a function of temperature: a comparison with other work. Except where already indicated, M = Ar for ■ and M = H_2O for ●. OTW, Olschewski *et al.* (1966), direct measurement of dissociation rate from shock-tube work. The remainder are calculated from the rates of the reverse process: Flame work: DSW, Dixon-Lewis *et al.* (1964); HJ, Halstead & Jenkins (1969); MW, McAndrew & Wheeler (1962); RS, Rosenfeld & Sugden (1964).

Shock-tube work: G, Getzinger (1966); GB, Getzinger & Blair (1968); SB, Schott & Bird (1964).

Figure 7 also shows the agreement with the most recent work on flames by Halstead & Jenkins (1968, 1969) for values of $k_{-1,Ar}$ and k_{-1,H_2O} and with the previous values of k_{-1,H_2O} from the flame studies of Dixon-Lewis, Sutton & Williams (1964), McAndrew & Wheeler (1962), and Rosenfeld & Sugden (1964).

The extrapolated lines in figure 7 for the results of the present work can be represented by the equations:

$$k_{-1,Ar} = 7.5 \times 10^{23}\ T^{-2.6}\ \mathrm{cm^6\ mol^{-2}\ s^{-1}},$$

$$k_{-1,H_2O} = 1.5 \times 10^{25}\ T^{-2.6}\ \mathrm{cm^6\ mol^{-2}\ s^{-1}}.$$

The extent to which these equations correlate the previously determined individual rate constants lends confidence to their use over a fairly wide range of temperatures.

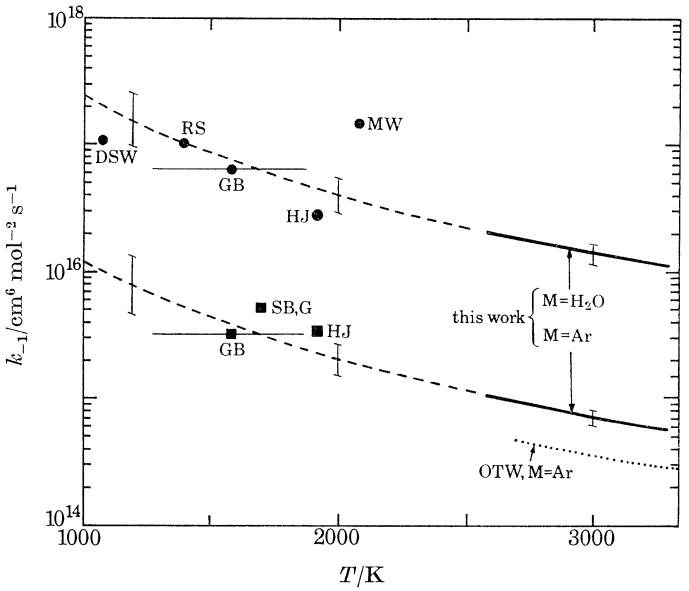

FIGURE 7. Rate constants for the reaction: $H + OH + M \rightarrow H_2O + M$, as a function of temperature: a comparison with other work. Symbols are the same as in figure 6. The error bars indicate the computed 95 % confidence limits on rate constants of this work.

7. CONCLUSIONS

We have shown that, at a temperature region of around 3000 K, the kinetics of the decomposition of water can be explained on the basis of the simple dissociation process of reaction (1), rather than be a peroxide mechanism which has been suggested previously. Water was found to be extremely efficient, compared to argon, in promoting the dissociation, and hence, by inference, also the recombination of H and OH. The rate constants determined for the dissociation process, and calculated for the reverse recombination process, when taken in conjunction with previous assessments in flames and shock tubes present a unified and most consistent set of rate data over a wide temperature range.

It is a pleasure to acknowledge the continued able assistance of Mr P. J. Swain with the experimental work.

REFERENCES

Appleton, J. P., Steinberg, M. & Liquornik, D. J. 1968 *J. chem. Phys.* **48**, 599.
Bauer, S. H., Schott, G. L. & Duff, R. E. 1958 *J. chem. Phys.* **28**, 1089.
Britton, D. 1960 *J. phys. Chem.* **64**, 742.
Christie, M. I., Harrison, A. J., Norrish, R. G. W. & Porter, G. 1955 *Proc. Roy. Soc. Lond.* A **231**, 446.
Dixon-Lewis, G., Sutton, M. M. & Williams, A. 1964 *Tenth Symp. (int.) Combustion*, p. 495. The Combustion Institute.
Engleman, R. 1969 *J. quant. Spectrosc. Radiat. Transfer* **9**, 391.

Garton, W. R. S. 1961 *Fifth (int.) Conf. Ionization Phenomena in Gases*, p. 1884. Amsterdam: North Holland.
Gaydon, A. G., Kimbell, G. H. & Palmer, H. B. 1963 *Proc. Roy. Soc. Lond.* A **276**, 461.
Getzinger, R. W. 1966 *Eleventh Symp. (int.) Combustion*, p. 117. The Combustion Institute.
Getzinger, R. W. & Blair, L. S. 1968 *Combust. Flame* **13**, 271.
Halstead, C. J. & Jenkins, D. R. 1968 *Twelfth Symp. (int.) Combustion* (to be published). The Combustion Institute.
Halstead, C. J. & Jenkins, D. R. 1969 *Combust. Flame*, to be published.
Hurle, I. R., Jones, A. & Rosenfeld, J. L. J. 1969 *Proc. Roy. Soc. Lond.* A **310**, 253.
Jenkins, D. R., Yumlu, V. S. & Spalding, D. B. 1966 *Eleventh Symp. (int.) Combustion*, p. 779. The Combustion Institute.
McAndrew, R. & Wheeler, R. J. 1962 *J. phys. Chem.* **66**, 229.
Olschewski, H. A., Troe, J. & Wagner, H. Gg. 1966 *Eleventh Symp. (int.) Combustion*, p. 155. The Combustion Institute.
Rosenfeld, J. L. J. & Sugden, T. M. 1964 *Combust. Flame* **8**, 44.
Schofield, K. 1967 *Planet. Space Sci.* **15**, 643.
Schott, G. L. & Bird, P. F. 1964 *J. chem. Phys.* **41**, 2869.
Troe, J. & Wagner, H. Gg. 1967 *Ber. Bunsenges. Physik. Chem.* **71**, 937.

PROCEEDINGS OF THE ROYAL SOCIETY A MATHEMATICAL, PHYSICAL & ENGINEERING SCIENCES